Using the Octree Immersed Boundary Method for urban wind CFD simulations

Available online at www.sciencedirect.com

ScienceDirect

IFAC PapersOnline CONFERENCE PAPER ARCHIVE

IFAC PapersOnLine 55-11 (2022) 179–184

Using the Octree Immersed Boundary Method for urban wind CFD simulations

R. Mitkov[§,*] **M. Pantusheva**[*] **V. Naserentin**[**,***]
P. O. Hristov[*,‡] **D. Wästberg**[****] **F. Hunger**[†] **A. Mark**[†]
D. Petrova-Antonova[*] **F. Edelvik**[†] **A. Logg**[**]

[*] *GATE Institute, Sofia University "St. Kliment Ohridski", Bulgaria*
[**] *Chalmers University of Technology, Sweden*
[***] *Aristotle University of Thessaloniki, Greece*
[****] *Chalmers Industiteknik, Sweden*
[†] *Fraunhoffer Chalmers Research Institute for Industrial Mathematics, Sweden*
[‡] *Institute for Risk and Uncertainty, University of Liverpool, UK*
[§] *Corresponding author: radostin.mitkov@gate-ai.eu*

Abstract: This paper describes the initial steps in a larger effort to perform verification and validation (V&V) of wind simulations in an urban environment. The presented work uses data from wind tunnel experiments on a simplified urban area to assess the performance of the steady-state RANS octree immersed boundary flow solver IBOFlow®. Verification and validation activities are indispensable in computational modelling, because they address the issue about the trustworthiness of models directly. This is particularly so in the modelling of complex systems such as urban environments. The results of the early V&V work are presented, together with a discussion on different aspects of the experimental and modelling settings. A key contribution of this work, which is planned as a first in a series of V&V publications, is the identification of concrete future actions to address the issues of trust in urban wind model predictions.

Keywords: CFD, RANS, Turbulence, Urban wind study, Immersed boundary method, Verification and validation

1. INTRODUCTION

The understanding of wind patterns in an urban environment is essential to ensuring a natural ventilation design and pedestrian wind comfort (Abd Razak et al., 2016; Blocken, 2015). In recent years, the increased number of densely-packed high-rise buildings in big cities has had a significant impact on ground level wind conditions (Dutt, 1991). As a result, numerous field measurements, wind tunnel tests and numerical simulations have been conducted to study these effects (Dutt, 1991; Blocken, 2015). Over the years, computational fluid dynamics (CFD) has been established as the numerical approach of choice for wind simulations, because it provides full-field characterisation of the flow, has considerable flexibility and the models do not suffer from any similarity constraints (Blocken, 2015). However, CFD models, just as any other computational model, must be treated with extreme care in order to obtain an accurate and reliable solution (Oberkampf and Trucano, 2002). Accuracy often depends upon the field of application - the acceptable error in some fields, e.g. aerospace engineering, could be less than 5%, while in others, such as wind engineering, it could be as high as 25% (Ferziger, 1990). Due to the various potential sources of numerical and physical modeling errors, validation and verification studies are crucial (Oberkampf and Roy, 2010).

This paper presents a preliminary verification and validation study of a steady-state flow solver developed for wind engineering purposes. The rest of the paper is organised as follows. Section 2 describes the IBOFlow® solver and some of the governing equations it is based on. Section 3 outlines the utility of validation and verification and describes the experimental setup used to validate the model presented in Section 4. Section 5 discusses the main results of the paper. The paper concludes with some closing remarks and provides some pointers for future work in Section 6.

2. FLOW SOLVER

For the simulations conducted in this paper, the steady-state solver in IBOFlow® (Immersed Boundary Octree Flow Solver) (Mark et al., 2011), developed at Fraunhofer-Chalmers Research Centre, was used. For the successful initialization of the simulation, an XML file, containing

⋆ This work is part of the Digital Twin Cities Centre supported by Sweden's Innovation Agency Vinnova under Grant No. 2019-421 00041, and GATE Project supported by the Horizon 2020 WIDESPREAD-2018-2020 TEAMING Phase 2 Programme under Grant Agreement No. 857155, the Swedish Research Council for Sustainable Development Formas (grants 2019-01169 and 2019-01885) and by Operational Programme Science and Education for Smart Growth under Grant Agreement No. BG05M2OP001-1.003-0002-C01. P.O. Hristov was funded by the National Scientific Program "Petar Beron i NIE" under the AUDiT project, no. KP-06-DB/3.

10.1016/j.ifacol.2022.08.069

details about the simulation setup, and a triangulated geometry file are necessary. The solver assumes an incompressible, isothermal flow governed by the Reynolds Averaged Navier-Stokes (RANS) equations:

Continuity:

$$\frac{\partial u_i}{\partial x_i} = 0 \tag{1}$$

Momentum:

$$\frac{\partial u_i}{\partial t} + u_j \frac{\partial u_i}{\partial x_j} = -\frac{1}{\rho}\frac{\partial p}{\partial x_i} + (\nu + \nu_t)\frac{\partial^2 u_i}{\partial x_j \partial x_j} - \frac{\partial\left(\frac{2}{3}K\delta_{ij}\right)}{\partial x_j} \tag{2}$$

where $\boldsymbol{u}$ is the mean velocity of the fluid, ρ is the fluid density, p is the dynamic pressure, ν is the kinematic viscosity of the fluid, ν_t is the eddy viscosity and K is the average kinetic energy of the velocity fluctuations. In addition, the immersed boundary (IB) condition is solved

$$u_i = u_i^{ib} \tag{3}$$

which constrains the velocity of the fluid to the velocity at the immersed boundary, u_i^{ib}. This is achieved through the implementation of the second-order accurate mirroring immersed boundary method (Mark and van Wachem, 2008).

All equations are discretised on a Cartesian octree grid using the finite volume method (Mark et al., 2011). The SIMPLEC method (Van Doormaal, 1984) is implemented for coupling the velocity and pressure fields, while the pressure-weighted flux interpolation (Rhie and Chow, 1983) prevents their decoupling. The steady-state solver employs artificial time stepping and solves until all relative matrix residuals are converged.

Closure of the RANS equations is achieved through the use of the $k-g$ SST (shear-stress transport) turbulence model (Kalitzin et al., 2005). It is based on the $k-\omega$ SST turbulence model and is derived by substituting the specific dissipation rate, ω, with the turbulence time scale $g = (C_\mu\omega)^{-1/2}$. The turbulent kinetic energy and turbulence time scale equations respectively are:

$$\frac{\partial k}{\partial t} + u_i\frac{\partial k}{\partial x_i} = P - \frac{k}{g^2} + \frac{\partial}{\partial x_i}\left[(\nu + \sigma_k\nu_t)\frac{\partial k}{\partial x_i}\right] \tag{4}$$

$$\frac{\partial g}{\partial t} + u_i\frac{\partial g}{\partial x_i} = -\alpha\frac{g}{2}P + \frac{\beta_1}{2gC_\mu} - (\nu + \sigma_g\nu_t)\frac{3}{g}\frac{\partial g}{\partial x_i}\frac{\partial g}{\partial x_i} + \frac{\partial}{\partial x_i}[(\nu + \sigma_g\nu_t)\frac{\partial g}{\partial x_i}] \tag{5}$$

where k is the turbulent kinetic energy, P is a production term. The eddy viscosity is defined as $\nu_t = C_\mu k g^2$, and $\sigma_k, \sigma_g, \alpha, \beta_1$ and C_μ are model constants. Similar to the $k-\omega$ SST turbulence model, the $k-g$ SST model resolves the flow using the $k-g$ formulation near the walls and $k-\epsilon$ in the free-stream.

3. EXPERIMENTAL WORK

This section discusses the need for verification and validation and the experimental setup used to gather data to support the validation effort.

3.1 Verification, validation and uncertainty quantification

All models in science and engineering, however elaborate and intricate they may be, are illustrations (see Box and Draper (1987)). The model cannot be made scientific merely by making it more complex, even when this complexity corresponds to real phenomena. This can only be done by careful uncertainty quantification (UQ). A crucial set of UQ activities, directly contributing the trustworthiness of models is that of verification and validation.

Verification is defined as the process of determining that a computer model implementation accurately represents the conceptual description of the model and the solution to that model (AIAA, 1998). In practical terms, verification deals with testing the reliability of the computer code, how well it represents the conceptual model of the processes under investigation, and estimating the error in the solution for the application of interest (Roy, 2005). Verification activities are documented in Section 5.1.

Verification work cannot determine if the model conforms well to reality. *Validation* is formally defined as the process of determining the degree to which a model is an accurate representation of the real world from the perspective of the intended uses of the model (AIAA, 1998). Validation is distinct from calibration and predictive capability estimation. Validation activities are discussed in Section 5.2.

3.2 The Architectural Institute of Japan (AIJ) Database

To be able to perform validation, a trustworthy source of information (a wind tunnel experiment or field measurements), reported with an adequate level of detail is needed. In this study, a public database provided by the Architectural Institute of Japan (AIJ) is selected to serve this purpose. This database contains benchmark test data for urban CFD wind simulations. It provides information for 13 different scenarios, starting from simple geometries such as single buildings, and gradually increasing the complexity to an actual urban area. The AIJ database is widely used as a source of validation data for urban wind simulations (see e.g. Li et al., 2018; Liu et al., 2018).

3.3 Validation case description - AIJ Case D

The case selected for this study is Case D from the AIJ Database [1]. It represents a simplified urban area with 83 buildings in total - one high-rise building in the centre (25 m × 25 m × 100 m in the x, y, and z directions, respectively), surrounded by an array of low-rise urban buildings (40 m × 40 m × 10 m each). The low-rise buildings are grouped in sectors separated by 10 m, 20 m and 30 m wide roads (Fig. 1). This geometry (1 : 400 scale) was used to conduct a series of wind tunnel experiments for varying wind directions (0°, 22.5°, and

[1] Available at `https://www.aij.or.jp/jpn/publish/cfdguide/index_e.htm`

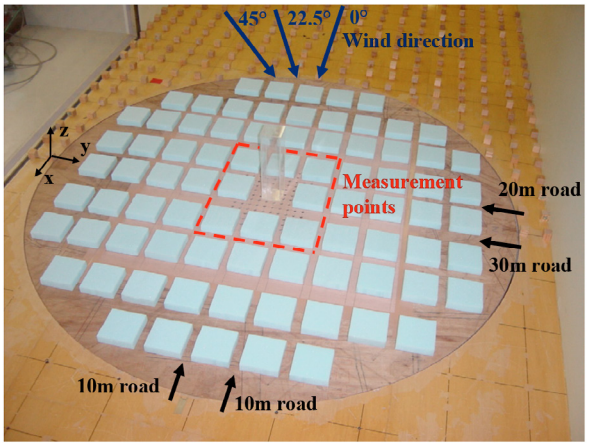

Fig. 1. Model geometry, Case D (image adapted from AIJ (2016), Photo 3-2-1).

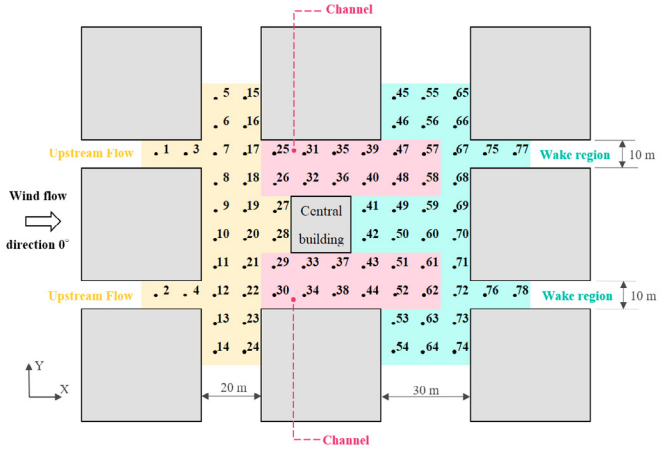

Fig. 2. Measurement points, Case D, AIJ

45°). The velocity field was measured at 78 different points located as shown in Fig. 2.

4. CFD MODEL

A model of Case D from the AIJ database is created for a CFD analysis using the in-house flow solver, IBOFlow®, developed at Fraunhofer-Chalmers Research Centre. Further details regarding the computational model are presented in the following sections.

4.1 Geometry

The geometry for the CFD model is created based on the CAD files provided by the AIJ Database [1]. The CFD model scale is the same as that of the experiment. The urban blocks are positioned in a box-shaped computational domain with dimensions 3.85 m × 6.40 m × 1.50 m in the x, y, and z directions. The domain dimensions are selected based on the best practice guidelines for urban CFD wind simulations (Franke et al., 2007; Tominaga et al., 2008; Blocken and Carmeliet, 2004; Blocken et al., 2016) and with respect to optimisation between accuracy and required computational resources. A general view of the domain with the offsets from the buildings to the domain boundaries measured in terms of the height of the central building is presented in Fig. 3.

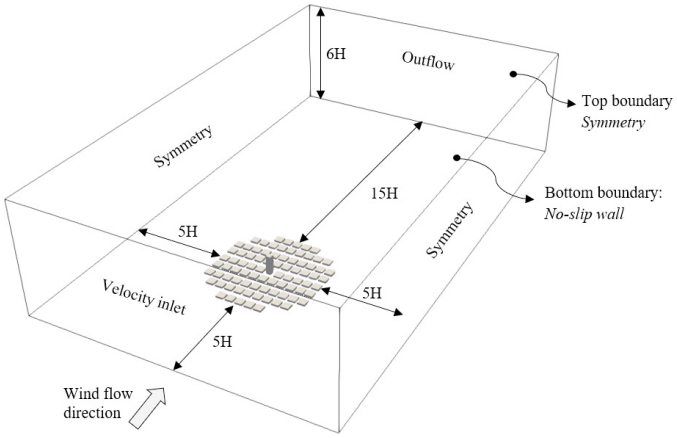

Fig. 3. Computational domain and boundary conditions, Case D, AIJ

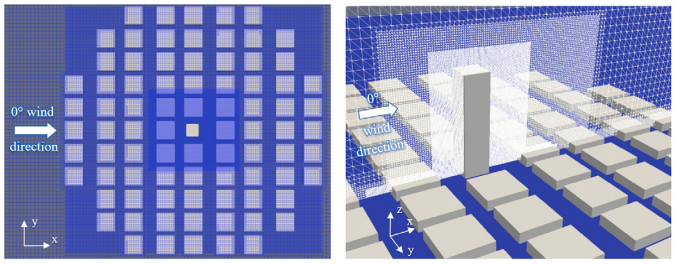

(a) (b)

Fig. 4. Medium mesh domain discretisation: (a) plan view; (b) three-dimensional section view

4.2 Discretisation

In this study, the immersed boundary method, described in Section 2 and native to IBOFlow® is used. The domain is discretised using a base grid with a maximum cell size of $0.08H$ (x) × $0.08H$ (y) × $0.08H$ (z), where H is the height of the central building. Three refinement levels (all with a ratio of 1 : 2) are applied to this base grid for finer discretisation in the areas of interest, namely in the region around the measurement points, extended to the front and wake regions of the central building as shown in Fig. 4. The mesh generated in this manner is a high-quality octree grid which consists purely of hexahedral cells.

A grid convergence study is presented in Section 5.1.

4.3 Boundary conditions

A summary of the boundary conditions is presented in Fig. 3. The inlet boundary is defined as a velocity inlet with profiles for velocity, turbulent kinetic energy, and dissipation rate, taken from the AIJ Database [1]. The horizontal wind velocity at the top level of the central building is $U_H = 6.61$ m/s.
The outflow is a zero pressure Dirichlet boundary condition. The top and side walls of the domain are modelled with symmetry boundary conditions. This assumption can be considered acceptable, because the minimum distances from the buildings to the domain boundaries, as defined in the best practice guidelines (Tominaga et al., 2008; Franke et al., 2007), would ensure undisturbed flow development. The building walls are modelled as no-slip smooth walls,

and the ground floor is represented by a no-slip wall condition with a sand grain height equal to 1.075×10^{-4} m as prescribed in the wind tunnel experiment, (AIJ, 2016).

4.4 Physics and turbulence modelling

In this paper the 0° wind case is investigated. The CFD simulations are carried out under the assumption of an incompressible, isothermal flow. A steady state solver is used based on the finite volume method incorporating the RANS equations, as described in Section 2. The third order QUICK convective scheme (Versteeg and Malalasekera, 2007) is selected for this study as an optimal choice in terms of application requirements and correlation to the experimental results. The choice of residual convergence limit is discussed in Section 5.1.

4.5 Simulation setup and calculation metrics

Five different cases based on Case D are investigated to explore different discretisation levels, and residual convergence limits. The outline of the simulations with the key settings for each case is presented in Table 1.

5. RESULTS AND DISCUSSION

This section describes the verification and validation results of applying IBOFlow®to predict the velocity field around the Case D wind tunnel model introduced in Section 3.3. In all of the plots presented in this section, the velocity magnitude has been normalized by the velocity at the central building height, $U_H = 6.61$ m/s.

5.1 IBOFlow® solution verification

Solution verification should be performed for every distinct application of the model. In the process, five types of errors are estimated, namely spatial and temporal discretisation error, iterative convergence error, statistical error and round-off error. In the case of the steady-state simulations described in Section 4, disregarding temporal discretisation error is admissible. Statistical error is irrelevant, since the model is deterministic and round-off error can be neglected due to the use of double-precision arithmetic in all computations. Thus, only spatial discretisation and iterative convergence error are treated here. One commonly applied method for dealing with spatial discretisation error is the so-called grid convergence study.

In this paper three grids with a different level of detail are investigated - coarse, medium, and fine. The base mesh for the three different studies is the same but it is refined at a different number of levels and therefore the minimum cell size in the areas of interest varies. The general mesh setup is described in Section 4.2 and summarised in Table 1. The narowest roads in the areas of interest are divided into 5, 10, and 20 elements, for the coarse, medium, and fine grids, respectively. Following the wind tunnel experiment, all results are reported at pedestrian height (2 m in real scale, or 0.005 m in the model scale).

Three progressively finer meshes were compared. Figure 5 depicts a comparison between the normalized velocities at each of the measurement locations for the three types of

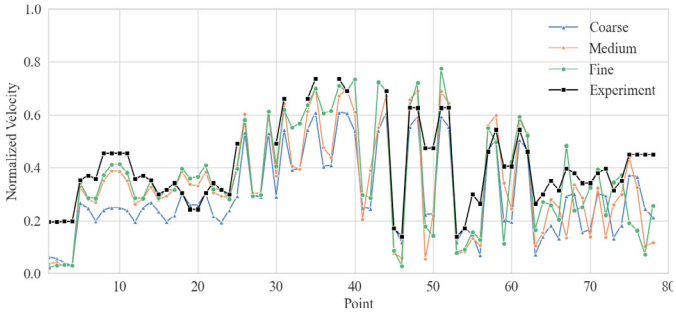

Fig. 5. Grid convergence study results

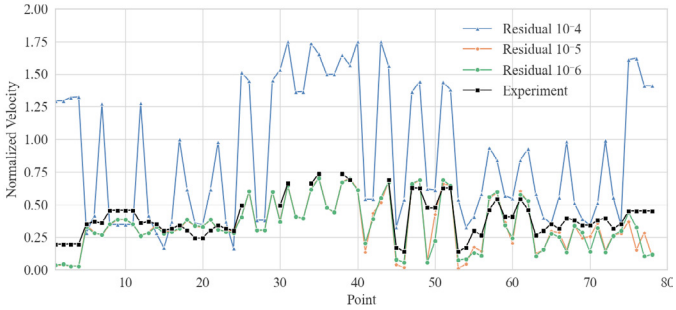

Fig. 6. Iterative convergence study results

grids - coarse, medium and fine. Examining the results, it can be seen that there is no significant difference between velocities in the channels (location depicted in Fig. 2), computed with the medium and fine grids so we can conclude that the solution is close to grid convergent. At the same time the fine grid has over three times as many elements as the medium one and so the medium grid was used in subsequent simulations.

To assess the magnitude of the iterative convergence error, three separate studies are conducted on the medium grid, varying the residual tolerance threshold on all conserved properties, between 1×10^{-4} and 1×10^{-6}. Figure 6 shows a plot similar to that for the mesh convergence. Comparing the three traces, it becomes clear that at residual level of 1×10^{-4}, the flow has not developed fully, as allowing the residuals to decrease another order of magnitude has a strong effect on the majority of velocity predictions. On the other hand, the change in velocity from simulations run to a residual level of 1×10^{-5} is small in comparison to those that had residuals of 1×10^{-6}, across all measurement points. As a result, a residual of 1×10^{-5} is considered sufficient for performing further simulations, taking into account the computational resources and time available.

5.2 IBOFlow® validation

The preliminary validation presented in this paper relies on several assumptions whose relaxation is outlined in Section 6:

- Initial and boundary conditions of the empirical test are precisely known, deterministic values.
- Empirical observations are precise.
- Simulations are run with identical initial and boundary conditions, and geometry to those used in the experiment.

Table 1. Outline of simulations. Minimum mesh size is identical in all directions. Pedestrian height given in mesh cell number, counting from the ground level up.

Mesh	Refinement levels	Minimum mesh size	Total number of cells	Pedestrian height	Residuals
Coarse mesh	2	5.0×10^{-3} m	5 769 108	between 1 and 2	1.0×10^{-5}
Medium mesh	3	2.5×10^{-3} m	7 024 523	between 2 and 3	1.0×10^{-4} 1.0×10^{-5} 1.0×10^{-6}
Fine mesh	4	1.25×10^{-3} m	17 093 897	between 4 and 5	1.0×10^{-5}

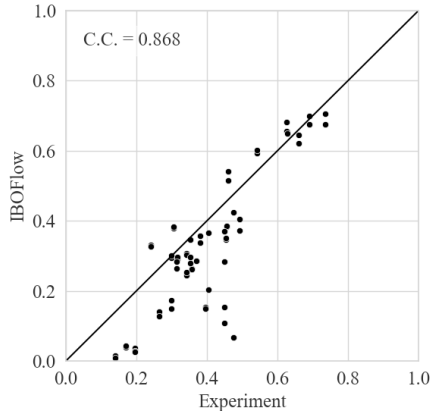

Fig. 7. Scatter plot of normalised velocities. Solid black line indicates perfect correspondence between predictions and observations.

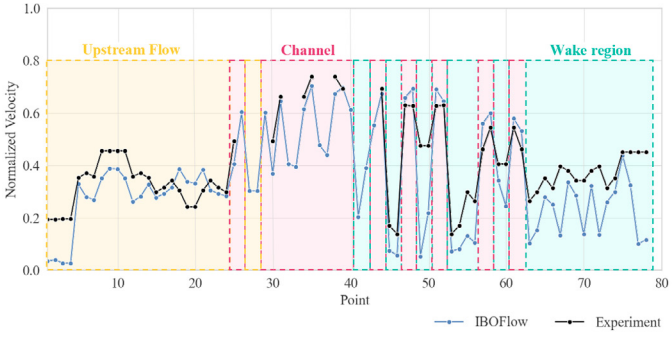

Fig. 8. Solution validation - normalized velocity at measurement points

The solution can be qualitatively validated by examining the conformity between the predicted and the measured velocity at each of the experimental points. Such a comparison is shown in Figure 7. There, the 45° line indicates a perfect correspondence between the data sets. It can be seen that the majority of the points lie in close proximity to this line. The correlation coefficient's value of 0.868 (labeled as 'C.C.' in Figure 7) between the computational and experimental data sets confirms the good agreement between the results. To gain further insight into the performance of the model, the normalized velocity plot, as seen from Figure 8 has been divided into regions in accordance to the regions depicted in Figure 2. Examining this plot, it can be noticed that the flow in the channel region, where wind velocity is the highest, shows only slight discrepancies when compared against the wind tunnel data. The most problematic region has proven to be the wake region. This is, however, expected as this is the area where the most unsteady flow structures occur.

Overall, the mesh convergence and validation results show that IBOFlow®is capable of capturing the flow properties in regions with relatively high velocity induced by the presence of a high-rise building. However, evidence shows that the model may not be able to provide accurate results in regions of unsteady, low-speed flow. There are two main avenues that could be explored to understand this behaviour and explore potential solutions. The first is to selectively refine the mesh in the wake region of the geometry to resolve more of the flow features. Such a step is supported by the grid convergence study which indicates the wake region has not converged. The second avenue for improvement is to consider the experimental data more closely. Experimental measurement errors and the actual wind tunnel model geometry, if provided, may result in an improved agreement between experiment and observation.

6. CONCLUSIONS

In this study, numerical simulations of wind flow in an urban context were carried out. A steady-state RANS solver with $k - g$ SST turbulence model was used to predict the wind velocity around a high-rise building surrounded by an array of low-rise housing. The computational results were compared to experimental data from the AIJ database. Solution verification in terms of grid and iterative convergence was performed, and solution validation proved that the main flow structures could be captured with adequate precision. The obtained results suggest that the wind velocity closely fits the experimental data in the high-velocity region, whereas it is generally underestimated in the low-velocity upstream and the wake regions.

In the past decades researchers and engineers have increased the usage of CFD simulations in their day-to-day work in the field of urban wind studies. Despite the numerous benefits provided by the computational analysis, a significant amount of verification, validation, and uncertainty quantification (UQ) activities must be performed in order to obtain a trustworthy model that can reliably resolve and predict the investigated physical phenomena. Nevertheless, these activities, in their full spectrum and appropriate level of detail, are rarely applied in practice. This publication aims to lay the foundation for a more comprehensive research effort to establish a workflow for all the necessary V&V, and UQ analyses essential for urban wind simulations. A series of publications will explore the effects of different urban layouts, environmental conditions, turbulence models, convective schemes, and other modelling parameters.

ACKNOWLEDGEMENTS

This work is part of the Digital Twin Cities Centre supported by Sweden's Innovation Agency Vinnova under Grant No. 2019-421 00041, and GATE Project supported by the Horizon 2020 WIDESPREAD-2018-2020 TEAMING Phase 2 Programme under Grant Agreement No. 857155, the Swedish Research Council for Sustainable Development Formas (grants 2019-01169 and 2019-01885), Operational Programme Science and Education for Smart Growth under Grant Agreement No. BG05M2OP001-1.003-0002-C01 and by Scientific Fund of Sofia University, agreement No. 80-10-11/10.05.2022. P.O. Hristov was funded by the National Scientific Program "Petar Beron i NIE" under the AUDiT project, no. KP-06-DB/3.

REFERENCES

Abd Razak, A., Hagishima, A., Awang Sa, Z.A., and Zaki, S.A. (2016). Progress in wind environment and outdoor air ventilation at pedestrian level in urban area. *Applied Mechanics and Materials*, 819, 236–240.

AIAA (1998). Guide for the verification and validation of computational fluid dynamics simulations. Technical report, American Institute of Aeronautics and Astronautics, AIAA-G-077–1998, Reston, VA.

AIJ (2016). AIJ Benchmarks for Validation of CFD Simulations Applied to Pedestrian Wind Environment around Buildings Architectural Institute of Japan. Technical report, Architectural Institute of Japan (AIJ), Tokyo, Japan.

Blocken, B., Stathopoulos, T., and van Beeck, J.P. (2016). Pedestrian-level wind conditions around buildings: Review of wind-tunnel and cfd techniques and their accuracy for wind comfort assessment. *Building and Environment*, 100, 50–81.

Blocken, B. (2015). Computational fluid dynamics for urban physics: Importance, scales, possibilities, limitations and ten tips and tricks towards accurate and reliable simulations. *Building and Environment*, 91, 219–245.

Blocken, B. and Carmeliet, J. (2004). Pedestrian wind environment around buildings: Literature review and practical examples. *Journal of Thermal Envelope and Building Science*, 28, 107–159.

Box, G.E.P. and Draper, N.R. (1987). *Empirical Model-Building and Response Surfaces*. John Wiley & Sons.

Dutt, A.J. (1991). Wind flow in an urban environment. *Environmental Monitoring and Assessment*, 19, 495–506.

Ferziger, J.H. (1990). Approaches to turbulent flow computation: Applications to flow over obstacles. *Journal of Wind Engineering and Industrial Aerodynamics*, 35, 1–19. doi:10.1016/0167-6105(90)90208-T.

Franke, J., Hellsten, A., Schlünzen, H., and Carissimo, B. (2007). Best Practice Guideline for the Cfd Simulation of Flows in the Urban Environment. Cost 732: Quality Assurance and Improvement of Microscale Meteorological Models. Technical report, Meteorological Institute, University of Hamburg, Hamburg, Germany.

Kalitzin, G., Medic, G., Iaccarino, G., and Durbin, P. (2005). Near-wall behavior of rans turbulence models and implications for wall functions. *Journal of Computational Physics*, 204, 265–291.

Li, J., Delmas, A., Donn, M., and Willis, R. (2018). Validation and comparison of different cfd simulation software predictions of urban wind environment based on aij wind tunnel benchmarks. In *Proceedings of the Symposium on Simulation for Architecture and Urban Design (SIMAUD '18)*.

Liu, J., Niu, J., Du, Y., and Mak, C. (2018). Large eddy simulation on the pedestrian level wind around a building community: Evaluation of influencing factors. In *Proceedings of the 4th International Conference on Building Energy, Environment, Melbourne, Australia*, 5–9.

Mark, A., Rundqvist, R., and Edelvik, F. (2011). Comparison between different immersed boundary conditions for simulation of complex fluid flows. *Fluid Dynamics and Materials Processing*, 7, 241–258.

Mark, A. and van Wachem, B.G. (2008). Derivation and validation of a novel implicit second-order accurate immersed boundary method. *Journal of Computational Physics*, 227, 6660–6680.

Oberkampf, W.L. and Roy, C.J. (2010). *Verification and Validation in Scientific Computing*. Cambridge University Press.

Oberkampf, W. and Trucano, T. (2002). Verification and validation in computational fluid dynamics. *Progress in Aerospace Sciences*, 38, 209–272.

Rhie, C.M. and Chow, W.L. (1983). Numerical study of the turbulent flow past an airfoil with trailing edge separation. *AIAA Journal*, 21, 1525–1532.

Roy, C.J. (2005). Review of code and solution verification procedures for computational simulation. *Journal of Computational Physics*, 205(1), 131–156.

Tominaga, Y., Mochida, A., Yoshie, R., Kataoka, H., Nozu, T., Yoshikawa, M., and Shirasawa, T. (2008). AIJ guidelines for practical applications of CFD to pedestrian wind environment around buildings. *Journal of Wind Engineering and Industrial Aerodynamics*, 96(10-11), 1749–1761.

Van Doormaal, J.P.and Raithby, G. (1984). Enhancements of the simple method for predicting incompressible fluid flows.

Versteeg, H. and Malalasekera, W. (2007). *An Introduction to Computational Fluid Dynamics. The finite volume method*. Pearson Education Limited.